439 25. **Lo KC, Brugh III VM, Parker M, Lamb DJ.** Isolation and enrichment of murine
440 spermatogonial stem cells using rhodamine 123 mitochondrial dye. *Biol Reprod* 2005; 72:
441 767-771.
442 26. **Nagano M, Avarbock MR, Brinster RL.** Pattern and kinetics of mouse donor spermatogonial
443 stem cell colonization in recipient testes. *Biol Reprod* 1999; 60: 1429-1436.
444 27. **Lo KC, Lei Z, Rao ChV, Beck J, Lamb DJ.** De novo testosterone production in luteinizing
445 hormone receptor knockout mice after transplantation of Leydig stem cells. *Endcrinology* 2004;
446 145:4011-4015.
447 28. **Yoshida S.** Casting back to stem cells. *Nat Cell Biol* 2009; 11: 118-120.
448 29. **Morimoto H, Kanatsu-Shinohara M, Takashima S, Chuma S, Nakatsuji N, Takehashi M,**
449 **Shinohara T.** Phenotypic plasticity of mouse spermatogonial stem cells. *PLos One* 2009; 4:
450 e7909.
451 30. **Wu Z, Luby-Phelps K, Bugde A, Molyneux LA, Denard B, Li W-H, Süel GM, Garbers DL.**
452 Capacity for stochastic self-renewal and differentiation in mammalian spermatogonial stem cells.
453 *J Cell Biol* 2009; 187: 513-524.
454 31. **Morita Y, Ema H, Yamazaki S, Nakauchi H.** Non-side-population hematopoietic stem cells in
455 mouse bone marrow. *Blood* 2006; 108: 2850-2856.
456 32. **Sato T, Laver JH, Ogawa M.** Reversible expression of CD34 by murine hematopoietic stem
457 cells. *Blood* 1999; 94:2548-2554.
458 33. **Klein AM, Nakagawa T, Ichikawa R, Yoshida S, Simons BD.** Mouse germ line stem cells
459 undergo rapid and stochastic turnover. Cell Stem Cell 2010; 7: 214-224.
460
461

461 **Figure Legends**

462

463 Figure 1. SP cell phenotype of GS cells. (A) RT-PCR analysis of transporter gene expression
464 demonstrating that GS cells express *Mrp*1, *Mrp4*, *Mrp5* and *Abcg*2. (B) EGFP-expressing GS cells
465 on a laminin-coated dish exhibit strong green fluorescence under UV light (inset). (C) Flow
466 cytometric analysis of GS cells stained with Hoechst 33342. GS cells were imaged by using filters
467 for Hoechst red and Hoechst blue emission. Whereas some of the GS cell cultures contained
468 Hoechst 33342-excluding cells (SP cells; left), other did not (right). (D) Inhibition of SP cell
469 development by verapamil. After GS cells were dissociated, the recovered cells were stained with
470 Hoechst 33342 in the absence (left) or presence (right) of verapamil. (E) Absence of SP cells in a
471 population of GS cells stably expressing active *Akt*. Bar = 50 μm (B).

472

473 Figure 2. Phenotypes of SP cells in GS cell culture. (A) Expression of surface markers on SP and
474 non-SP cells. The black-shaded area indicates control staining. No significant differences between
475 SP and non-SP cells are evident. (B) Rh 123 efflux characteristics of SP and non-SP cells. GS cells
476 from ROSA26 mice were stained with Hoechst 33342 and Rh 123.

477

478 Figure 3. Functional analyses of SP cells in GS cell culture. (A) Reversibility of the SP cell
479 phenotype. GS cells cultured on laminin-coated dishes were sorted into SP and non-SP cells
480 according to their Hoechst 33342 staining patterns. The SP and non-SP cells were cultured for 29
481 and 34 days in vitro and stained again with Hoechst 33342. (B) Macroscopic appearance of recipient
482 W testes transplanted with SP (right) and total EGFP-expressing cells (left). Approximately 0.2-1.3
483 $\times 10^3$ SP or 1.0-2.4 $\times 10^3$ non-SP cells were transplanted into each testis. Green fluorescence
484 indicates colonization by donor cells. (C) Histological appearance of the recipient testes. W testes

485 transplanted with SP cells produce colonies undergoing normal spermatogenesis (right). In contrast,
486 non-transplanted W testes demonstrate no evidence of ongoing spermatogenesis (left). Bars = 50 μm
487 (A), 1 mm (B) and 100 μm (C).
488
489 Figure 4. SP cell analysis after transplantation of WT GS cells. (A) A diagram showing the
490 experimental strategy. EGFP-expressing GS cells were transplanted into the primary W recipient
491 mice. Some of the recipients were made cryptorchid to eliminate differentiated germ cells. Recipient
492 testes were dissociated at early (7-14 days) or late (3-4 months) phases after transplantation and
493 stained with Hoechst 33342. After cells expressing EGFP were gated, SP and total EGFP-expressing
494 cells in the EGFP-expressing cell population were sorted and transplanted into secondary W
495 recipients. (B) Comparison of light-scattering properties (left) and EGFP fluorescence (right) of
496 dispersed testis cells from WT and cryptorchid recipients. Donor-derived cells were gated based on
497 EGFP fluorescence and side scatter for SP cell identification. (C) Comparison of Hoechst 33342
498 staining patterns of dispersed testis cells from WT and cryptorchid recipients. (D) Expression of
499 surface markers on SP and non-SP cells in WT W recipients. The black-shaded area indicates
500 control staining. (E) Macroscopic appearance of recipient testes that were transplanted with SP (top)
501 and total EGFP-expressing cells (bottom). Approximately 0.7-2.0 × 10^3 SP or 3.2-7.0 × 10^4 non-SP
502 cells were transplanted into each testis. Green fluorescence indicates colonization by donor cells.
503 Bar = 1 mm (E).
504
505 Figure 5. SP cell analysis after transplantation of *H-RasV12*-transfected GS cells into W testes. (A)
506 Macroscopic (left) and histological (right) appearance of a recipient testis transplanted with
507 *H-RasV12*-transfected GS cells. Arrows indicate abnormal germ cell clumps in the seminiferous
508 tubules; arrowheads indicate invasion into interstitial tissue. Note the abnormal spermatogenesis in

509 the seminiferous tubules. (B) Light-scattering properties (left) and EGFP fluorescence (right) of
510 dispersed testis cells from recipients that were transplanted with *H-RasV12*-transfected cells.
511 Donor-derived cells were gated based on EGFP fluorescence and side scatter for SP cell
512 identification. (C) Hoechst 33342 staining patterns of dispersed testis cells from recipient testes that
513 were transplanted with *H-RasV12*-transfected cells. Although SP cells were found in total testis cells
514 (left) and in EGFP-expressing testis cells (right), the overall pattern of Hoechst 33342 staining was
515 significantly different from that observed after transplantation of WT GS cells (see Fig. 4C). (D)
516 Macroscopic appearance of recipient testes transplanted with SP (left) and total EGFP-expressing
517 cells (right). Approximately 0.6-5.9 $\times$ 10^3 SP or 0.6-3.0 $\times$ 10^4 non-SP cells were transplanted into
518 each testis. Green fluorescence indicates colonization by donor cells. Bars = 100 μm (A, right) and 1
519 mm (A, left; D).
520
521
522

Table 1. Summary of transplantation experiments

Experiment	Donor cells	No. of experiments	No. of cells injected[a]	No. of testes injected	No. of testes colonized (%)	No. of colonies /testis/10^5 cells[b]	*P* value by t-test
In vitro	SP	4	150-1300	20	8 (40)	560.3 ± 432.0	0.12
	Total EGFP	4	1000-2400	20	16 (80)	142.5 ± 22.6	
In vivo (WT)	SP	3	650-2000	18	0 (0)	0	0.40
	Total EGFP	3	32000-70000	16	3 (19)	0.8 ± 0.4	
In vivo (Ras)	SP	3	640-5900	17	2 (12)	10.1 ± 9.1	0.30
	Total EGFP	3	5900-30000	17	2 (12)	0.5 ± 0.3	

Values are means±SEM.

[a]Approximate number of cells was calculated by assuming 4 μl of cells was transplanted.

[b]Number of individual colonies in each testis. Results were normalized to 10^5 cells injected/testis.

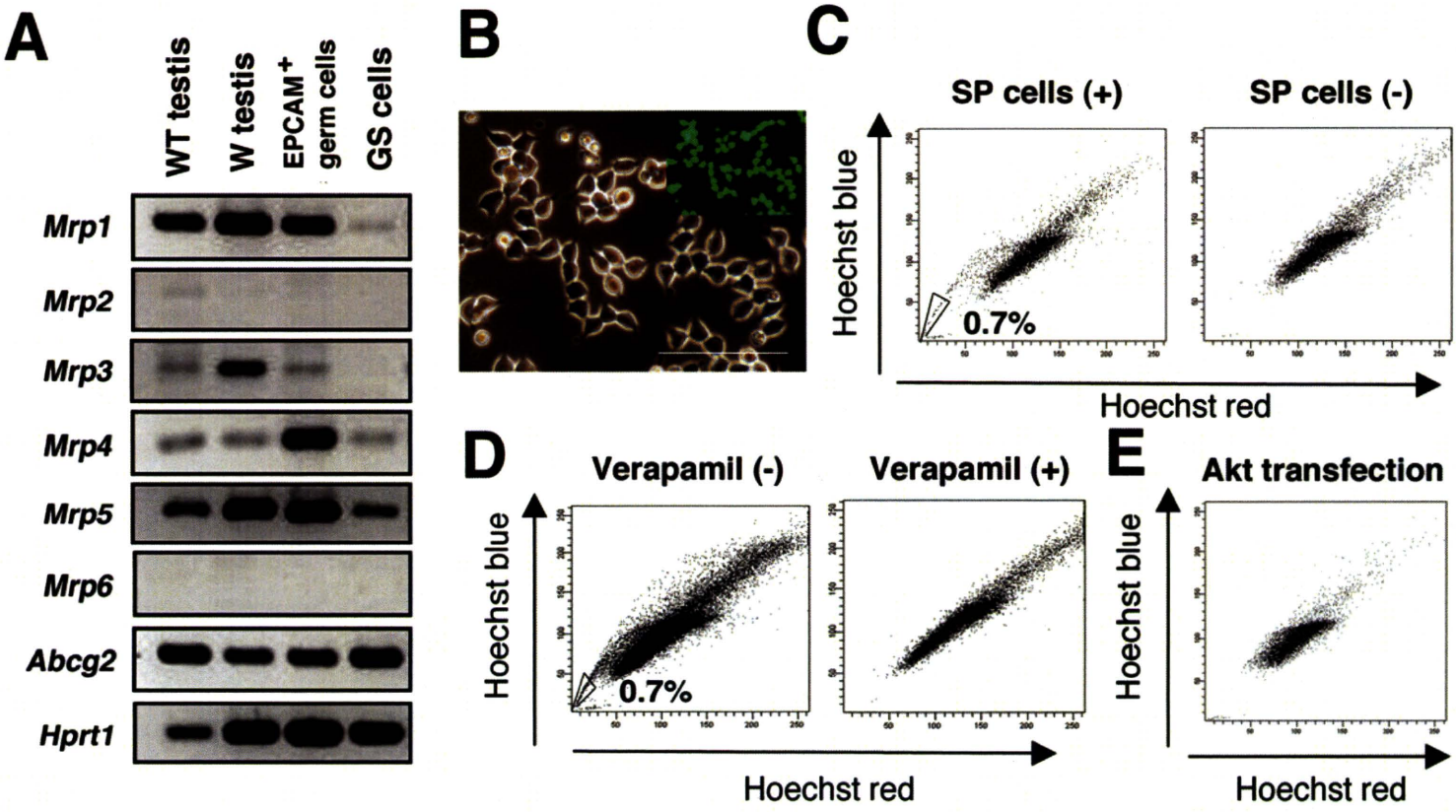

Figure 1. SP cell phenotype of GS cells. (A) RT-PCR analysis of transporter gene expression, demonstrating that GS cells express *Mrp*1, *Mrp4*, *Mrp5*, and *Abcg*2. (B) EGFP-expressing GS cells on a laminin-coated dish exhibit strong green fluorescence under UV light (inset). (C) Flow cytometric analysis of GS cells stained with Hoechst 33342. GS cells were imaged by using filters for Hoechst-red and Hoechst-blue emission. Whereas some of the GS cell cultures contained Hoechst 33342-excluding cells (SP cells; left), other did not (right). (D) Inhibition of SP cell development by verapamil. After GS cells were dissociated, the recovered cells were stained with Hoechst 33342 in the absence (left) or presence (right) of verapamil. (E) Absence of SP cells in a population of GS cells stably expressing active *Akt*. Bar = 50 μm (B).

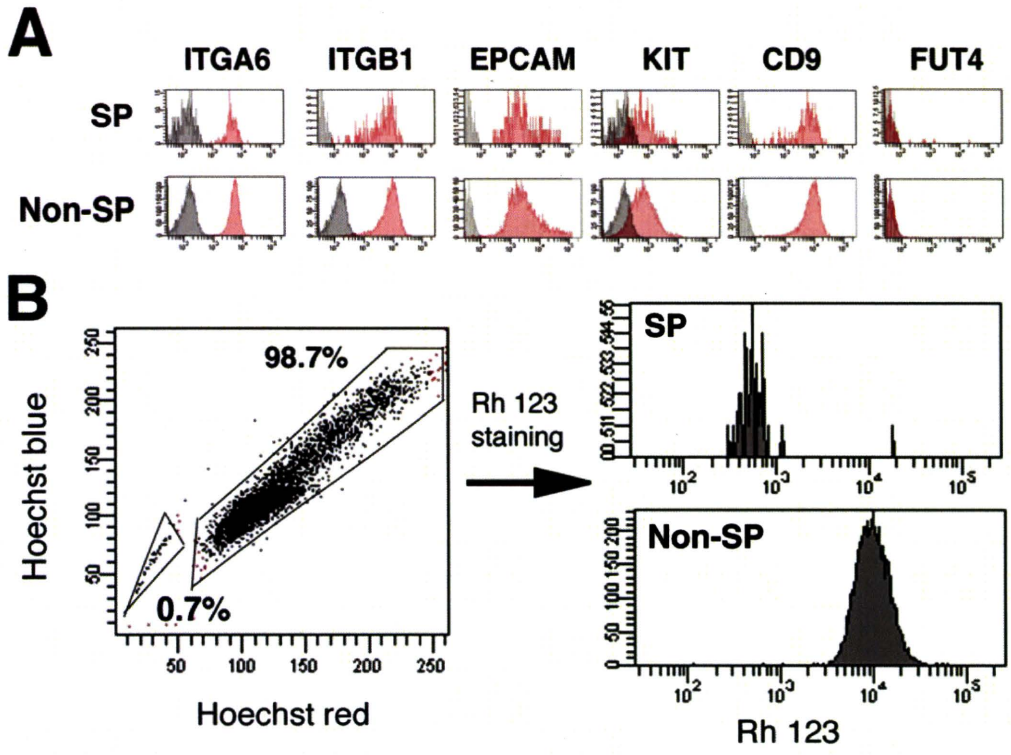

Figure 2. Phenotypes of SP cells in GS cell culture. (A) Expression of surface markers on SP and non-SP cells. The black-shaded area indicates control staining. No significant differences between SP and non-SP cells are evident. (B) Rh 123 efflux characteristics of SP and non-SP cells. GS cells from ROSA26 mice were stained with Hoechst 33342 and Rh 123.

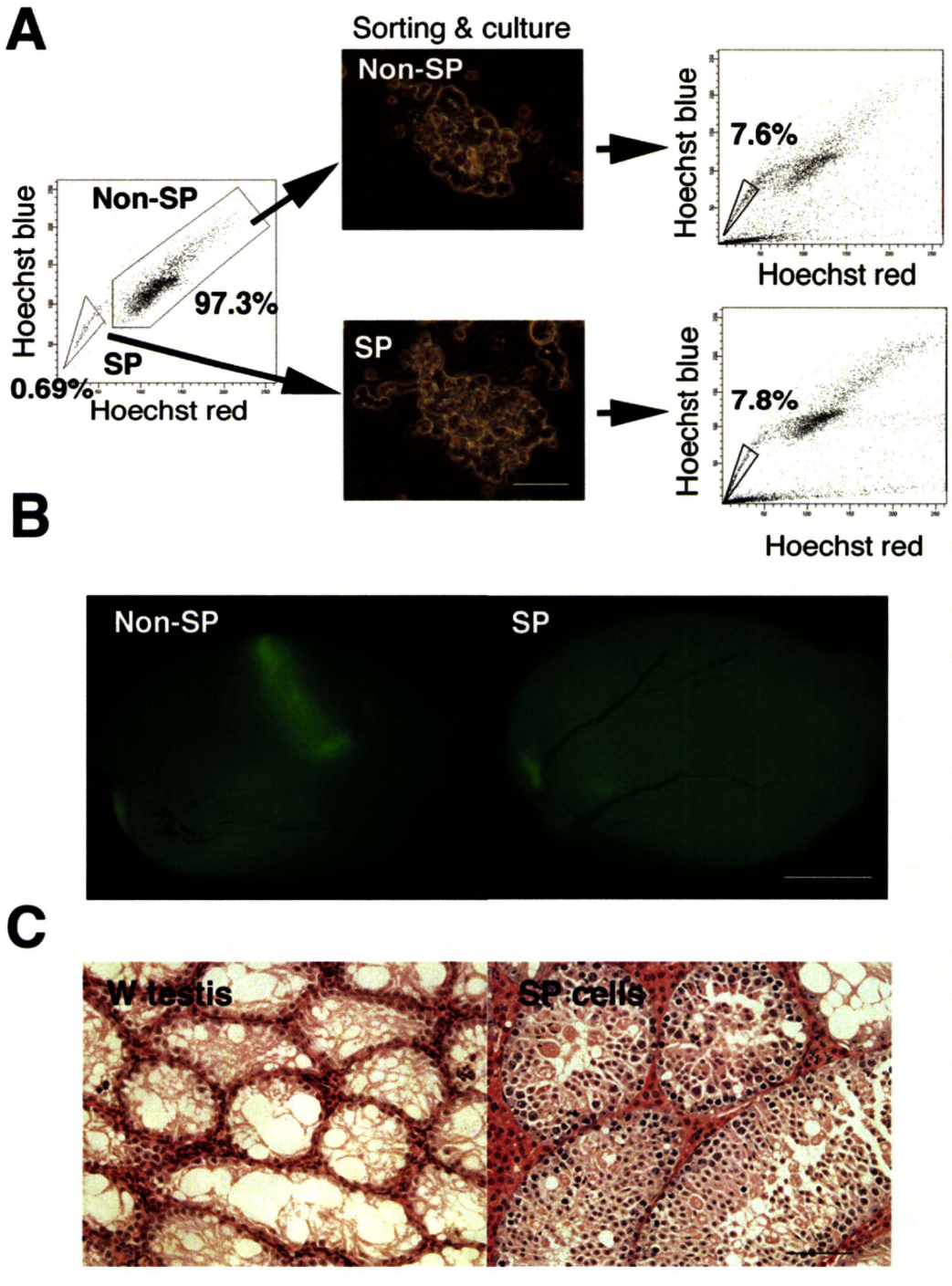

Figure 3. Functional analyses of SP cells in GS cell culture. (A) Reversibility of the SP cell phenotype. GS cells cultured on laminin-coated dishes were sorted into SP and non-SP cells according to their Hoechst 33342 staining patterns. The SP and non-SP cells were cultured for 29 and 34 days in vitro and stained again with Hoechst 33342. (B) Macroscopic appearance of recipient W testes transplanted with SP (right) and total EGFP-expressing cells (left). Approximately 0.2-1.3 × 10^3 SP or 1.0-2.4 × 10^5 non-SP cells were transplanted into each testis. Green fluorescence indicates colonization by donor cells. (C) Histological appearance of the recipient testes. W testes transplanted with SP cells produce colonies undergoing normal spermatogenesis (right). In contrast, non-transplanted W testes demonstrate no evidence of ongoing spermatogenesis (left). Bar = 50 μm (A); 1 mm (B); 100 μm (C).

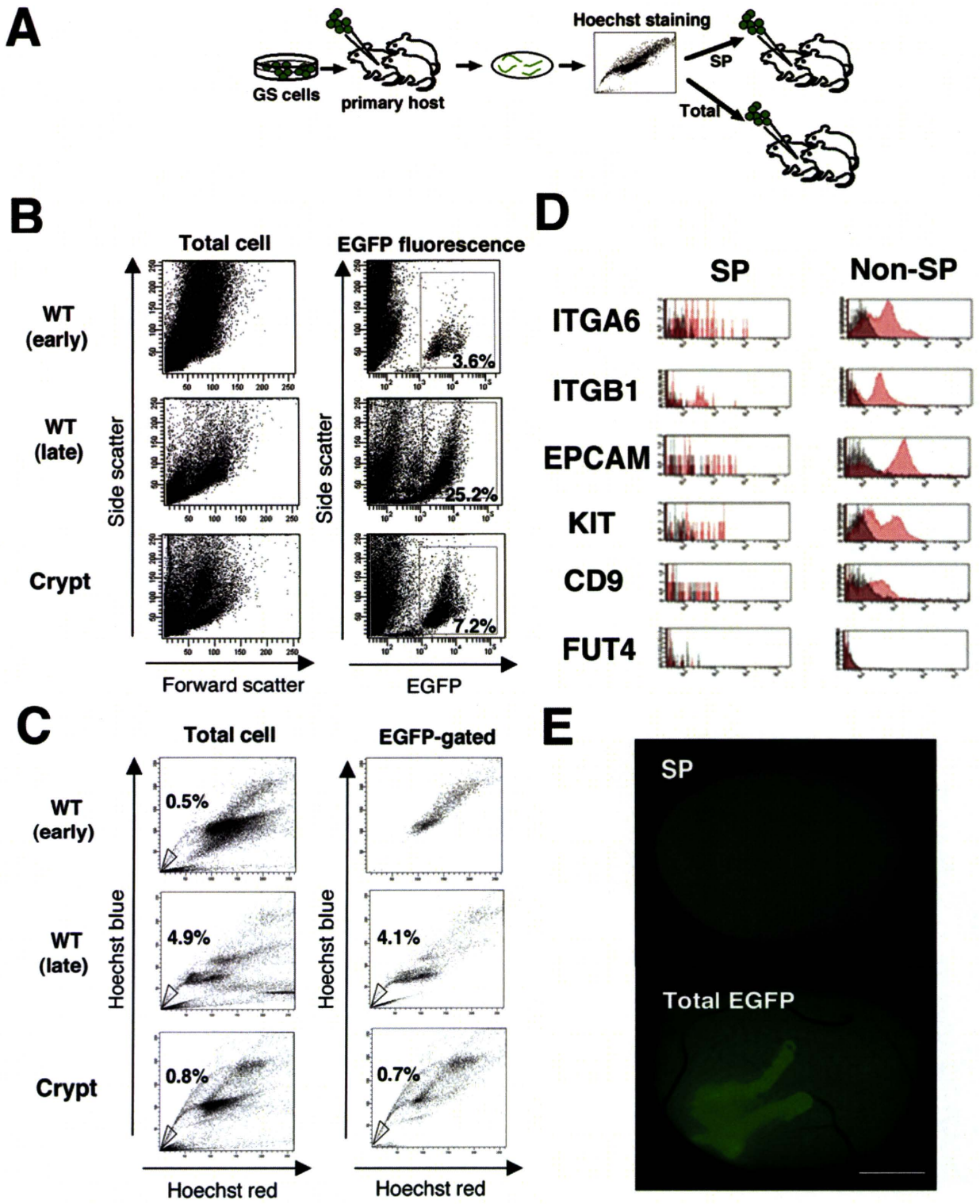

Figure 4. SP cell analysis after transplantation of WT GS cells. (A) A scheme showing the experimental strategy. EGFP-expressing GS cells were transplanted into the primary W recipient mice. Some of the recipients were made cryptorchid to eliminate differentiated germ cells. Recipient testes were dissociated at early (7-14 days) or late (3-4 months) phases after transplantation and stained with Hoechst 33342. After cells expressing EGFP were gated, SP and total EGFP-expressing cells in the EGFP-expressing cell population were sorted and transplanted into secondary W recipients. (B) Comparison of light-scattering properties (left) and EGFP fluorescence (right) of dispersed testis cells from WT and cryptorchid recipients. Donor-derived cells were gated based on EGFP fluorescence and side scatter for SP cell identification. (C) Comparison of Hoechst 33342 staining patterns of dispersed testis cells from WT and cryptorchid recipients. (D) Expression of surface markers on SP and non-SP cells in WT W recipients. The black-shaded area indicates control staining. (E) Macroscopic appearance of recipient testes that were transplanted with SP (top) and total EGFP-expressing cells (bottom). Approximately 0.7-2.0 × 10^3 SP or 3.2-7.0 × 10^4 non-SP cells were transplanted into each testis. Green fluorescence indicates colonization by donor cells. Bar = 1 mm (E).

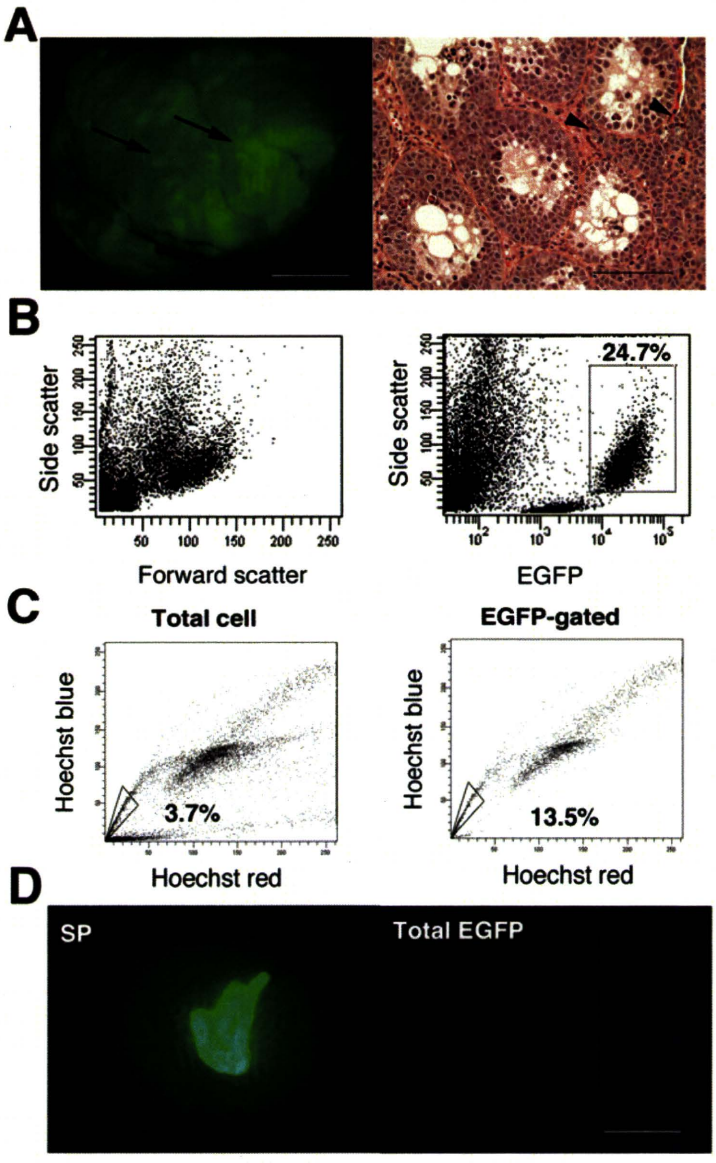

Figure 5. SP cell analysis after transplantation of *H-RasV12*-transfected GS cells into W testes. (A) Macroscopic (left) and histological (right) appearance of a recipient testis transplanted with *H-RasV12*-transfected GS cells. Arrows indicate abnormal germ cell clumps in the seminiferous tubules; arrowheads indicate invasion into interstitial tissue. Note the abnormal spermatogenesis in the seminiferous tubules. (B) Light-scattering properties (left) and EGFP fluorescence (right) of dispersed testis cells from recipients that were transplanted with *H-RasV12*-transfected cells. Donor-derived cells were gated based on EGFP fluorescence and side scatter for SP cell identification. (C) Hoechst 33342 staining patterns of dispersed testis cells from recipient testes that were transplanted with *H-RasV12*-transfected cells. Although SP cells were found in total testis cells (left) and in EGFP-expressing testis cells (right), the overall pattern of Hoechst 33342 staining was significantly different from that observed after transplantation of WT GS cells (see Fig. 4C). (D) Macroscopic appearance of recipient testes transplanted with SP (left) and total EGFP-expressing cells (right). Approximately 0.6-5.9 × 10^3 SP or 0.6-3.0 × 10^4 non-SP cells were transplanted into each testis. Green fluorescence indicates colonization by donor cells. Bar = 100 μm (A, right); 1 mm (A, left; D).

Biochemical and Biophysical Research Communications 400 (2010) 27–33

Contents lists available at ScienceDirect

Biochemical and Biophysical Research Communications

journal homepage: www.elsevier.com/locate/ybbrc

Neonatal mouse testis-derived multipotent germline stem cells improve the cardiac function of acute ischemic heart mouse model

Toru Iwasa [a], Shiro Baba [a,*], Hiraku Doi [a], Shinji Kaichi [a], Noritaka Yokoo [a], Takahiro Mima [a], Mito Kanatsu-Shinohara [b], Takashi Shinohara [b,1], Tatsutoshi Nakahata [a], Toshio Heike [a]

[a] Department of Pediatrics, Graduate School of Medicine, Kyoto University, 54 Kawahara-cho, Shogoin, Sakyo-ku, Kyoto 606-8507, Japan
[b] Department of Molecular Genetics, Graduate School of Medicine, Kyoto University, Konoe-cho, Yoshida Sakyo-ku, Kyoto 606-8501, Japan

ARTICLE INFO

Article history:
Received 29 July 2010
Available online 4 August 2010

Keywords:
mGS
Flk1
Cardiac regeneration therapy

ABSTRACT

Multipotent germline stem (mGS) cells have been established from neonatal mouse testes. We previously reported that undifferentiated mGS cells are phenotypically similar to embryonic stem cells and that fetal liver kinase 1 (Flk1)$^+$ mGS cells have a similar potential to differentiate into cardiomyocytes and endothelial cells compared with Flk1$^+$ embryonic stem cells. Here, we transplanted these Flk1$^+$ mGS cells into an ischemic heart failure mouse model to evaluate the improvement in cardiac function. Significant increase in left ventricular wall thickness of the infarct area, left ventricular ejection fraction and left ventricular maximum systolic velocity was observed 4 weeks after when sorted Flk1$^+$ mGS cells were transplanted directly into the hearts of the acute ischemic model mice. Although the number of cardiomyocytes derived from Flk1$^+$ mGS cells were too small to account for the improvement in cardiac function but angiogenesis around ischemic area was enhanced in the Flk1$^+$ mGS cells transplanted group than the control group and senescence was also remarkably diminished in the early phase of ischemia according to β-galactosidase staining assay. In conclusion, Flk1$^+$ mGS cell transplantation can improve the cardiac function of ischemic hearts by promoting angiogenesis and by delaying host cell death via senescence.

1. Introduction

The main cause of severe heart failure is ischemic heart disease. Although heart transplantation is the most effective therapy for end-stage severe heart failure, demand of donor hearts far outstrips supply of available hearts [1]. To this end, cardiac stem/progenitor cells are considered as one of promising source for radical cell-based therapies to bridge ischemic heart disease patients to or altogether replace heart transplantation [2–6].

Several studies reported that embryonic stem (ES) cells are one of hopeful cell source for transplantation into heart and improvement of cardiac function had observed by the transplantation of ES cells. Because ES cell are derived from fertilized eggs, there is ethical problem in establishment of human ES cells and application for human therapy. Furthermore ES cells are derived from other individuals, there is also immunological problem of host rejection to the transplanted cells.

Recently multipotent germline stem (mGS) cells were established from neonatal mouse testis. The mGS cells have less ethical problem compared with ES cells and if the mGS cells are established from an ischemic heart disease patient and the mGS cells are applied for treatment of the patient, we can provide novel and better cell therapy for ischemic heart disease with less ethical and immunological problem.

We previously reported that mGS cells from neonatal mouse testis are as favorable as mouse ES cells for differentiation into cardiomyocytes and endothelial cells by the selection with the mesodermal cell surface marker [7,8], fetal liver kinase 1 (Flk1) [9,10]. The differentiated cardiomyocytes derived from mGS cells have similar electrophysiology as adult mouse cardiomyocytes *in vitro* [10]. Furthermore, we reported that Flk1$^+$ cells derived from ES cells have the potential to improve cardiac function in a model of cardiomyopathy by direct cardiac transplantation [5]. Given these convincing results, we transplanted Flk1$^+$ cells derived from mGS cells directly into acute ischemic hearts, and evaluated the improvement in cardiac function. Moreover, we studied the effect of Flk1$^+$ mGS cell-transplantation on cardiac regeneration.

Abbreviations: mGS cells, multipotent germline stem cells; Flk1, fetal liver kinase 1; ES cells, embryonic stem cells; FCS, fetal calf serum; 2ME, 2-mercaptoethanol; LIF, leukemia inhibitory factor; LAD, left anterior descendant coronary artery; LVDd, left ventricular end-diastolic diameter; LVEF, left ventricular ejection fraction; +dP/dt, maximum systolic velocity change; −dP/dt, minimum diastolic velocity change; cTn-I, cardiac troponin-I; TUNEL, terminal deoxynucleotidyl transferase dUTP nick end labeling; AMI, acute myocardial infarct; iPS cells, induced pluripotent stem cells.

* Corresponding author. Fax: +81 75 752 2361.
E-mail addresses: shibaba@kuhp.kyoto-u.ac.jp (S. Baba), tshinoha@virus.kyoto-u.ac.jp (T. Shinohara).
[1] Fax: +81 75 751 4169.

0006-291X/$ - see front matter © 2010 Elsevier Inc. All rights reserved.
doi:10.1016/j.bbrc.2010.07.131

2. Materials and methods

2.1. Cell culture and differentiation

Green fluorescence protein positive mGS cells were maintained on mouse embryonic fibroblasts in DMEM (Sigma) containing 15% fetal calf serum (FCS) (Sigma), 1×10^{-4} M 2-mercaptoethanol (2ME) and 5000 U/ml leukemia inhibitory factor (LIF) as described previously [9,10]. These cells were differentiated into mesodermal cells on OP-9 stromal cell layers in alpha-MEM (Gibco) containing 10% FCS (Sigma) and 5×10^{-5} M 2ME without LIF (differentiation medium) at a concentration of 3×10^4 cells/25 cm^2 flask (FALCON) [10,11]. OP-9 cell line was a kind gift from Dr. Kodama and was maintained as described previously [12].

2.2. FACS Vantage sorting

The cell surface marker antibodies used in these FACS experiments were a rat anti-mouse Flk1 antibody (BD Pharmingen) [7] and allophycocyanin-conjugated anti-rat IgG antibody served as a secondary antibody. Analysis was performed by FACSCalibur (BD Biosciences). The mGS cell derivatives were divided into $Flk1^+$ and $Flk1^-$ cells by anti-Flk1 labeling followed by sorting with a FACSVantage SE (BD Biosciences) 4 days after differentiation.

2.3. β-Galactosidase assay

Cell-transplanted hearts were removed quickly on day 3 and day 7 after the cells transplantation, each heart coronal sections were incubated at 37 °C (no CO_2) with fresh senescence-associated β-galactosidase (3-Gal (SA-3-Gal) stain solution: 1 mg of 5-bromo-4-chloro-3-indolyl P3-D-galactoside (X-Gal) per ml/40 mM citric acid/sodium phosphate, pH 6.0/5 mM potassium ferrocyanide/5 mM potassium ferrocyanide/150 mM NaCl/2 mM $MgCl_2$ [13,14]. Staining was evident in 2–4 h and all the specimens were incubated for 6 h.

2.4. Transplantation of mGS cells to acute myocardial ischemic model mice

To produce acute myocardial ischemic model mice, we used 8-week-old male DBA/2 mice. As mGS cells were produced from these DBA/2 mice testes, the MHC types of this mouse and mGS cells are same. All animal handling procedures followed the Guide for the Care and Use of Laboratory Animals published by the US National Institutes of Health (NIH Publication No. 85–23, revised 1996) and the guidelines of the Animal Research Committee of the Graduate School of Medicine, Kyoto University. Mice were anesthetized and intubated for mechanical controlled ventilation before thoracotomy. After opening their left intercostal space, left anterior descendant coronary artery (LAD) was ligated permanently. The 10 μl of $Flk1^+$ or $Flk1^-$ mGS cells suspension (3×10^5/10 μl) was then injected dividedly into two sites of marginal zone (between scar area and normal area). The number of mice were as follows, $n = 10$ for $Flk1^+$ mGS cells transplantation, $n = 5$ for $Flk1^-$ mGS cells transplantation, $n = 14$ for medium injection (sham group), $n = 10$ for non-treatment (control group).

2.5. Hemodynamic measurements and electrocardiogram recordings

Hemodynamics was indirectly measured via echocardiography with a 15–16 MHz phased-array transducer (model 21390A, PHILIPS). Left ventricular diastolic diameter (LVDd) and left ventricular systolic diameter were measured and the left ventricular ejection fraction (LVEF) was calculated as previously described [2]. Cardiac catheterization was performed 4 weeks after the cell transplantation by using a 1.4-Fr micro manometer tipped catheter (Miller Instruments Inc.). Left ventricular pressure curve was recorded and left ventricular maximum systolic velocity (+dP/dt) and minimum diastolic velocity (−dP/dt) were calculated by a PowerLab System (PowerLab 4/25 ML845 and BIO Amp CF ML132) (ADInstruments) [5]. All measurements were performed under anesthesia with mask inhalation of 0.5–1.0% sevoflurane and a heart rate of approximately 450/min.

2.6. Histology

Tissue slices (7 μm) were fixed with 4% paraformaldehyde and incubated with antibodies specific for the following markers: cardiac troponin-I (cTn-I) (Santa Cruz Biotechnology), CD31 (Becton Dickinson), p53 (BD Pharmingen) and p21 (BD Pharmingen). Cy3-conjugated donkey anti-mouse IgG, Cy3-conjugated donkey anti-goat IgG, and Cy3-conjugated goat anti-rat IgG (Jackson ImmunoResearch Laboratories, Inc.) served as secondary antibodies. All heart sections were incubated with these antibodies using the M.O.M. kit (Vector Laboratories, Inc.) to prevent non-specific reactions. Many heart slices were also stained with hematoxylin–eosin (HE) to detect abnormal cell growth due to transplanted $Flk1^+$ or $Flk1^-$ mGS cells. Hearts fixed in 10% formalin were embedded in paraffin, sectioned at 4 μm thickness, and stained with Masson-Trichrome for detecting fibrosis in infarcted areas. For apoptosis analysis, infarcted hearts were frozen in cryomolds, sectioned, and terminal deoxynucleotidyl transferase dUTP nick end labeling (TUNEL) was performed according to the manufacturer's protocol (*In Situ* Apoptosis Detection kit; Takara).

2.7. Statistical analysis

Data were analyzed with paired or unpaired two-tail Student's *t*-test with Microsoft Excel software. Statistical significance was defined as a p value of less than 0.05.

3. Results

3.1. Transplantation of $Flk1^+$ mGS cells significantly improves the cardiac function of ischemic hearts

We used 8-week-old male DBA/2 mice. Ten minutes after permanent LAD occlusion, 3×10^5 $Flk1^+$ mGS cells were transplanted equally into two sites of the anterior left ventricular free wall. As a control group, an equivalent volume of medium was injected into the AMI model mouse hearts in a similar fashion.

To investigate whether $Flk1^+$ mGS cells undergo cardiomyogenesis *in vivo* as efficiently as they do *in vitro* and whether cardiac function improves after $Flk1^+$ mGS cell transplantation, we sorted mGS-derived $Flk1^+$ cells on day 4 of differentiation (Fig. 1A). A total of 39 mice were used in these experiments as follows: 10 AMI model mice were transplanted with $Flk1^+$ mGS cells, 14 AMI model mice were injected with an equivalent volume of medium alone, and 10 normal mice were used as controls. In addition, we injected $Flk1^-$ mGS cells into hearts of 5 AMI model mice. To assess the severity of cardiomyopathy in the AMI model mice, LVDd and LVEF were assessed by echocardiography at weeks 0 and 4. Although the LVDd of the $Flk1^+$ mGS cell transplanted group and the medium injected group was not significantly different at 4 weeks after the cell transplantation, the $Flk1^+$ mGS cell transplanted group had significantly higher LVEF values than the medium injected group (Fig. 1B and C).

Cardiac catheterization in mice was used to evaluate the left ventricular +dP/dt and left ventricular −dP/dt parameters at 4 weeks

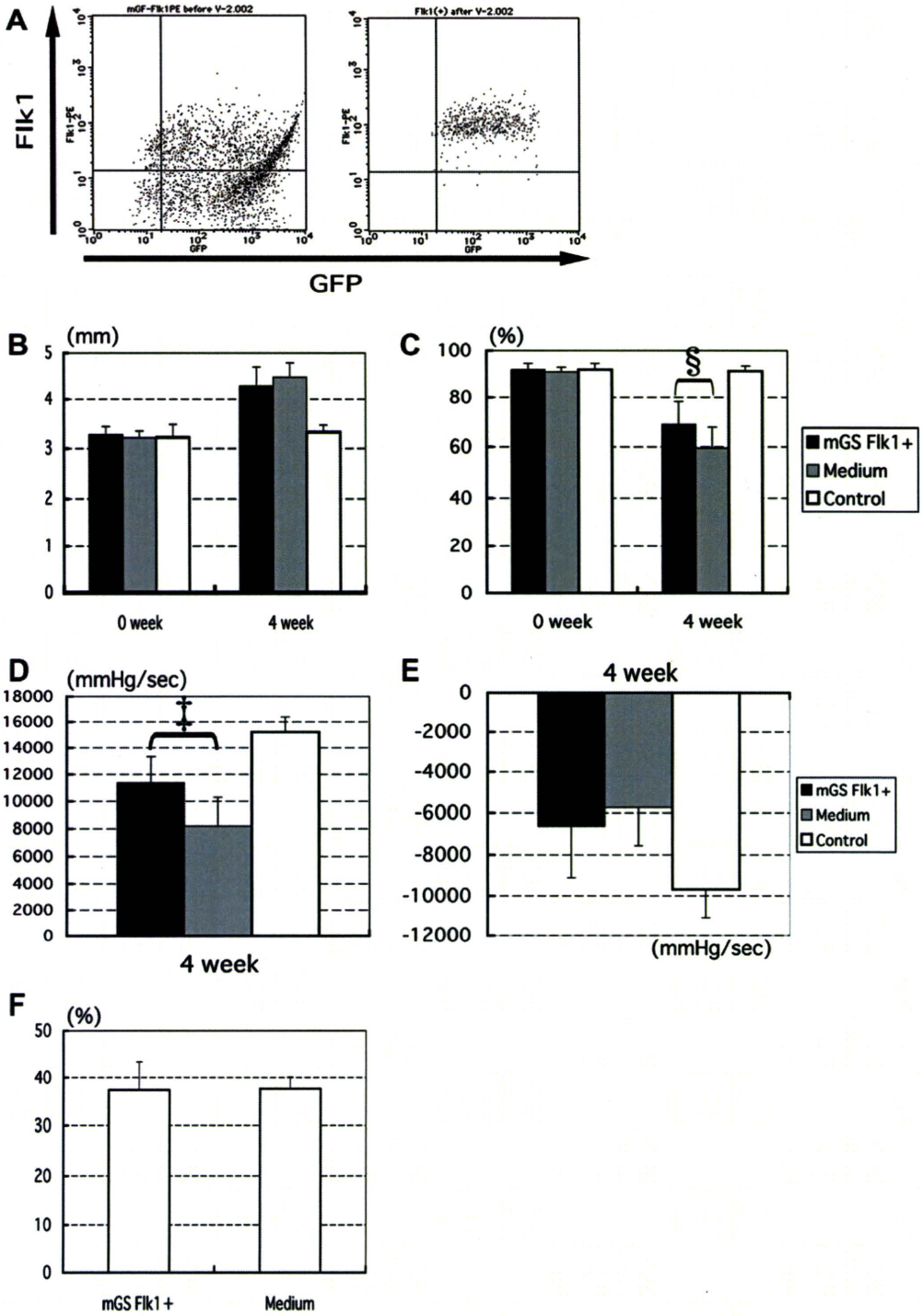

Fig. 1. (A) mGS cell-derived Flk1$^+$ cells were detected clearly after 4-day differentiation (left panel). Flk1$^+$ mGS cells were sorted by flow cytometry with greater than 97% purity (right panel). (B,C) The results of echocardiography in each group. LVDd between in the Flk1$^+$ mGS cell transplanted group and in the medium injected control group was not significantly different (B). LVEF between the Flk1$^+$ mGS cell transplanted group and the medium injected group was significantly different (C). (D,E) The results of cardiac catheterization in each group reveals that significant increase of +dP/dt in the Flk1$^+$ mGS cell transplant group, but not in the medium injected group. (F) The percentage of infarcted circumference was calculated in each group. $^{\ddagger}p < 0.01$, $^{\S}p < 0.05$.

after the cell transplantation. The Flk1$^+$ mGS cell transplanted group showed significant improvement in +dP/dt values when compared to the values of the medium injected group (Fig. 1D). As for −dP/dt, there were no significant difference between these two groups (Fig. 1E). These results indicated that Flk1$^+$ mGS cell transplantation was influenced by the systolic function, not diastolic function, of AMI model mouse hearts. Of course, the size of infarcted area (the ratio of infarcted circumference to the entire heart circumference) was not significantly different in each group as evaluated by Masson-Trichrome stain (Fig. 1F). In contrast, the cardiac function of Flk1$^-$ mGS cell transplanted group was not recovered 4 weeks after transplantation assessed by echocardiography and cardiac catheterization (LVDd 4.31 ± 0.41 mm, LVEF 57.6 ± 11.6%, +dP/dt 9167.4 ± 1722.2 mmHg/s, −dP/dt −5958.1 ± 1311.7 mmHg/s, respectively).

3.2. Flk1$^+$ mGS cells differentiated into cardiomyocytes and endothelial cells in AMI model mice heart

Cardiomyogenesis of the transplanted Flk1$^+$ mGS cells in AMI model mouse hearts was evaluated by immunohiostochemistory. Transplanted Flk1$^+$ mGS cells differentiated not only into cTn-I positive cardiomyocytes in the infarcted area but also endothelial cells that form tube-like structures (Fig. 2A and B). These differentiated cardiomyocytes and endothelial cells may partly contribute to the improvement of cardiac function.

To investigate another mechanism of the observed improved cardiac function with Flk1$^+$ mGS cell transplantation, we quantified the number of vessels in the marginal zone. The marginal zone was defined as the area between infarcted area and normal (non-ischemic) area. The number of the vessels, defined as tube-like structures with CD31 positive cells, was significantly higher in the Flk1$^+$ mGS cell transplanted group than that of the medium injected group (Fig. 2C). These results suggested that enhanced angiogenesis in the marginal zone should supply better blood flow in the Flk1$^+$ mGS transplanted group than in the medium injected group. In the hearts transplanted Flk1$^-$ mGS cells, we could not detect differentiated cardiomyocytes and endothelial cells derived from Flk1$^-$ mGS cells.

3.3. Preserved LV wall thickness in the marginal zone by the Flk1$^+$ mGS cells transplantation

In infarcted areas, we observed increased cardiomyocyte survival in the Flk1$^+$ mGS cell transplanted group than the medium injected group (Fig. 3A–D). The wall thickness of infarcted area was much thicker in the Flk1$^+$ mGS cell transplanted group than in the medium injected group (Fig. 3E). In contrast, the wall thickness of infarcted area in the Flk1$^-$ mGS cell transplanted group was same as that of the medium injected group.

3.4. Apoptosis in the marginal zone was not suppressed by the Flk1$^+$ mGS cells transplantation

To investigate the mechanism of cardiomyocyte survival, we first counted the number of apoptotic cells in the marginal zone of each group 0, 6, 12, and 24 h and 4 weeks by TUNEL staining after Flk1$^+$ cell transplantation or medium injection (Fig. 3F–H). The number of apoptotic cells rapidly increased 6 h after infarction and then gradually decreased until 24 h. The ratio of apoptotic cells to non-apoptotic cells 24 h after Flk1$^+$ mGS cell transplantation was almost the same as during the time course from 0 h to 4 weeks after Flk1$^+$ cell transplantation or medium injection (Fig. 3I). These results revealed that the observed apoptosis after infarction was not suppressed by Flk1$^+$ mGS cell transplantation compared to medium injection.

3.5. Senescence in the marginal zone was prevented and delayed by the Flk1$^+$ mGS cells transplantation

Next, we investigated the association of Flk1$^+$ mGS cell transplantation and senescence, a type of cell death [13,15,16]. Senescent cells were detected by a β-galactosidase assay 3 and 7 days after the Flk1$^+$ mGS cell transplantation and the medium injection. Although there were no significant difference in β-galactosidase stained areas between the Flk1$^+$ mGS cell transplanted group and

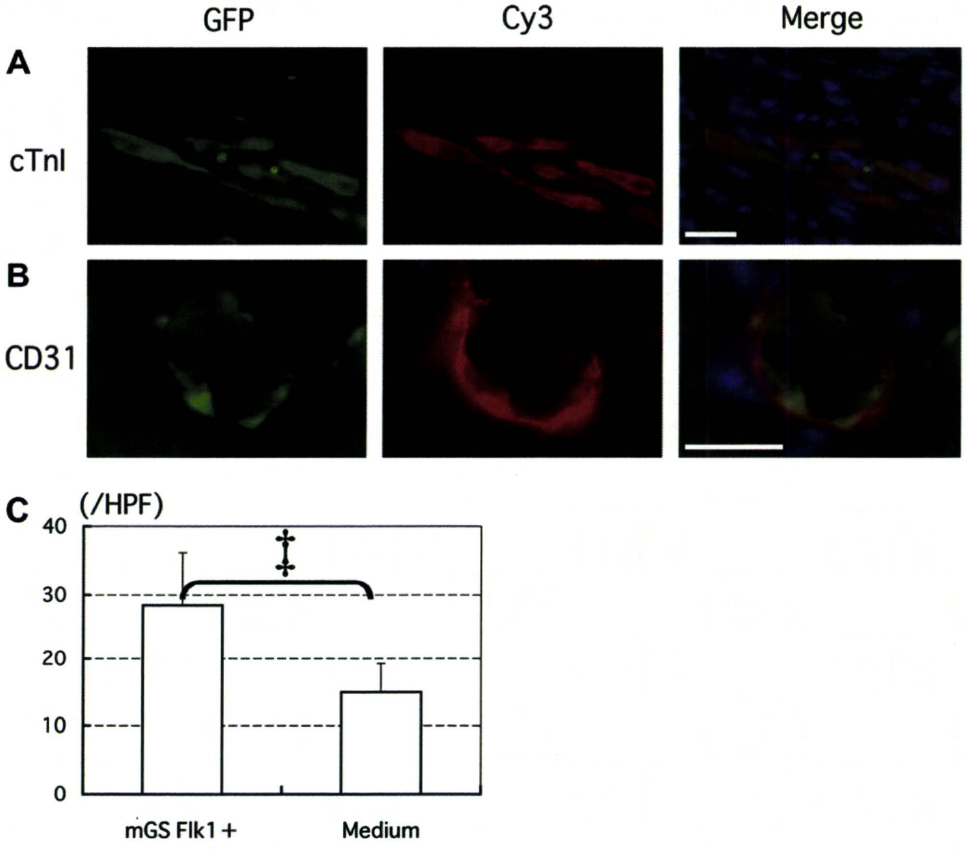

Fig. 2. (A) GFP$^+$ mGS cells (left, green) were stained with cardiac troponin-I (cTn-I) (middle, red). Merged image (right). (B) GFP$^+$ mGS cells with a tube structure (left panel, green) were stained with CD31 (middle panel, red). Merged image (right). The nuclei were counterstained with Hoechst 33342 (blue). (C) The number of CD31$^+$ vessels in the marginal zone in each group. Scale bar: 100 μm. ‡$p < 0.01$. (For interpretation of the references to colour in this figure legend, the reader is referred to the web version of this article.)

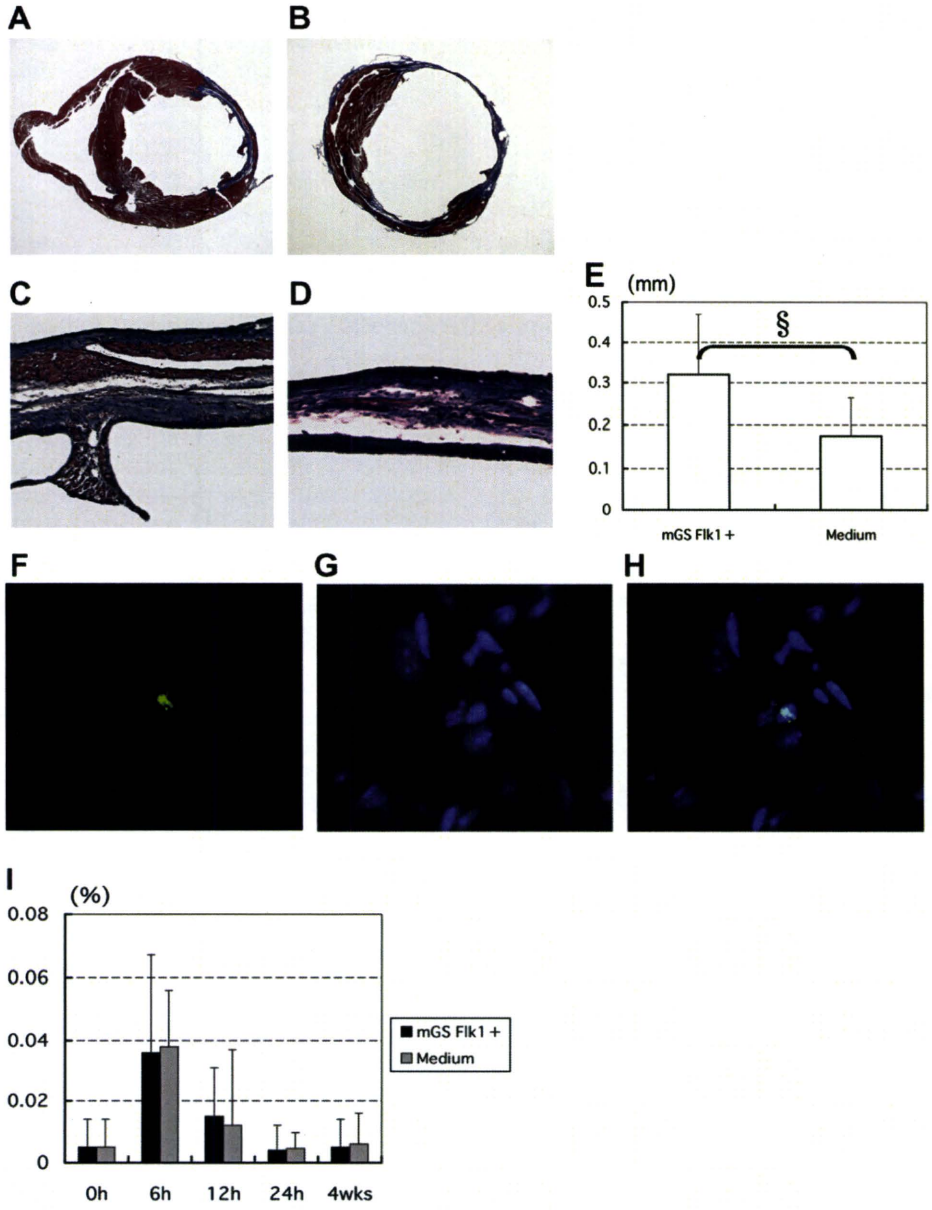

Fig. 3. (A) Coronal sections of Flk1$^+$ mGS cell transplanted heart 4 weeks after the cell transplantation. This section was stained with Masson-Trichrome stain. (C) A magnified area of infarcted area from panel A. (B) The coronal section of a medium injected heart 4 weeks after the injection. This section was stained with Masson-Trichrome stain. (D) The magnification of infarcted area in the panel B. (E) The thickness of the infarcted anterior wall in each group. $^{\S}p < 0.05$. (F–H) TUNEL positive nucleus (F: left, green) was detected in the marginal zone. The nuclei were counterstained with Hoechst 33342 (G: middle, blue). Merged image (H: right). (I) The percentages of TUNEL positive nuclei were compared after Flk1$^+$ mGS cell transplantation or control medium injection. There were no significant difference between the Flk1$^+$ mGS cell transplanted group and the medium injected group over the 4-week time course. (For interpretation of the references to colour in this figure legend, the reader is referred to the web version of this article.)

the medium injected group 7 days after the transplantation, the β-galactosidase stained area was undoubtedly smaller 3 days after the transplantation in the Flk1$^+$ mGS cell transplanted group than in the medium injection group (Fig. 4A–D). Especially in the Flk1$^+$ mGS cell transplanted group, the β-galactosidase stained area on days 3 was located in the endocardium side of infarcted area. On the other hand, the epicardium side of infarcted area was not stained deeply by the β-galactosidase (Fig. 4A). These results revealed that the cell dearth via the cell senescence was delayed by the Flk1$^+$ mGS cells transplantation. Finally, we investigated the cell signals, p21 and p53 that were elevated during the senescence pathway [17,18], to confirm that the senescence is actually prevented by the cells transplantation. Activated p21 and p53 were not clearly detected in the epicardium and endocardium sides of infarcted area in the Flk1$^+$ mGS cell transplanted group on 3 days after the cell transplantation (Fig. 4F and G). As to the medium injected group, activated p21 and p53 were clearly detected all layers from endocardium to epicardium in the infarcted area (Fig. 4H and I).

4. Discussion

There were a lot of candidates of cell sources for the cell transplantation to heart failure model animals [2–4,19–21]. In these sources, we reported the Flk1$^+$ mGS cells were one of the most convincing cell sources previously [10]. These Flk1$^+$ mGS cells have enough potential in their expansion at the undifferentiated state and in their differentiation into cardiomyocytes and endothelial cells *in vitro*. Under this knowledge, we transplanted these cells into the hearts of AMI model mice. Stem cells derived from various tissues including adipose tissue and bone marrow can also differenti-

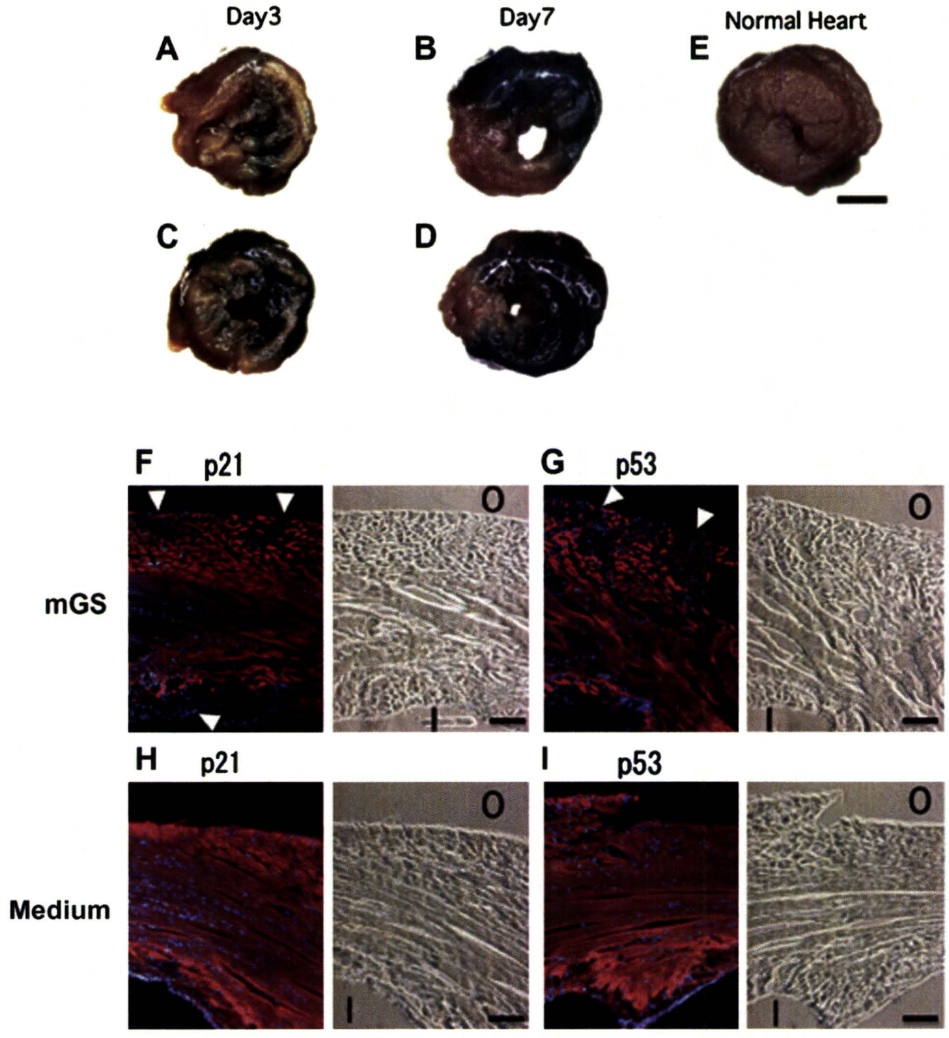

Fig. 4. (A–D) β-Galactosidase staining was detected 3 days (A) and 7 days (B) after Flk1$^+$ mGS cell transplantation. β-Galactosidase staining was also detected 3 days (C) and 7 days (D) after control medium injection. (E) β-Galactosidase staining was not detected in the non-ischemic normal heart. Scale bar: 1 mm. (F,G) Activated p21 and p53 were not clearly detected in the epicardium and endocardium of infarcted areas in Flk1$^+$ mGS cell-transplanted hearts (arrowheads). (H,I) Activated p21 and p53 were clearly detected in the epicardium and endocardium of the infarcted area in medium injected hearts. The nuclei were counterstained with Hoechst 33342 (blue). Bar; 50 μm. O, Outside the left ventricle. I, Inside the left ventricles. (For interpretation of the references to colour in this figure legend, the reader is referred to the web version of this article.)

ate into cardiomyocytes and endothelial cells *in vitro* and *vivo* [22], indeed, but judging from *in vitro* differentiation capacity, mGS cells, which have equal potential in differentiation into endothelial cells to ES cells, have much priority.

Furthermore, the use of mGS cells in cardiac regeneration therapy for ischemic heart disease has much advantage. In the pluripotent or multipotent stem cells, ES cells have ethical problem, adult stem cells have less differentiate potential into cardiomyocyte and endothelial cells than ES cells or mGS cells *in vitro*, and induced pluripotent stem (iPS) cells are consist of transgenes and have a problem to be oncogenic.

Transplantation of the Flk1$^+$ mGS cells improved the left ventricular systolic function and a part of Flk1$^+$ mGS cells could differentiate into cardiomyocytes and endothelial cells *in vivo*. But we could not be sure that only a few numbers of these differentiated cells were sufficient to bear the results of this cardiac functional improvement. However; if we can improve the method of transplantation, it is surely expected that the differentiation potential of Flk1$^+$ mGS into cardiomyocytes and endothelial cells can be remarkably increased *in vivo* compared to other tissue stem cells. In contrast, the Flk1$^-$ mGS cell transplantation did not improve the cardiac function of AMI model mice. And more, we could not detect any differentiated cardiomyocyte or endothelial cell derived from Flk1$^-$ mGS cells in the infarcted area.

Except for the cardiac and endothelial cells differentiation from the transplanted cells, the mechanisms of cardiac function improvement after the cell transplantation were reported previously. Some reported the mechanism was vasculogenesis [2,6,23], and others reported it was anti-apoptotic effect [2] after the cell transplantation for AMI models. In our experiments, the thickness of the infarcted area was significantly larger in the Flk1$^+$ mGS cell transplanted group than in the medium injected group. Simultaneously, angiogenesis in the marginal zone was more frequently detected in the Flk1$^+$ mGS cell transplanted group than that in the medium injected group. Most of these new vessels were not the result of regeneration from the transplanted Flk1$^+$ mGS cells, but the result of the angiogenesis from the host cells. These results indicate that the sufficient blood perfusion resulting from enough angiogenesis enables host cardiomyocytes to survive after Flk1$^+$ mGS cells transplantation. At this time, we questioned why angiogenesis is enhanced specifically after the Flk1$^+$ mGS cells transplantation and not after the medium injection. Furthermore, we investigated the cell death mechanism after cell transplantation. We first investigated the anti-apoptotic effect of cell transplantation. But the

anti-apoptotic effect was not clearly revealed by the TUNEL staining in our experiments. Gonzalez et al. previously reported that activation of cardiac progenitor cells reversed senescence and improved the cardiac function in the failing heart [16]. Because we think that the Flk1$^+$ mGS cells are similar to cardiac stem/progenitors cells, a similar phenomenon may occur after the Flk1$^+$ mGS cell transplantation. The reduction effect of senescence may occur in the transplantation of ES cells, adipose tissue stem cells or bone marrow derived cells, further examination is needed for selecting the most effective cells from these cell source and mGS cells. In the β-galactosidase assay, cell death via senescence was clearly inhibited at the early phase of AMI after the Flk1$^+$ mGS cells transplantation. In addition, the signals p21 and p53 were activated in senescent cells and both signals were especially inhibited around the epicardial layers in the infarcted area at the very early phase of AMI. From these results, Flk1$^+$ mGS cell transplantation first prevents cell senescence in infarcted areas at the very early phase of ischemia. Next, angiogenesis from transplanted cells was enhanced during this period. Finally, a number of original host cardiomyocytes survived in the Flk1$^+$ mGS cell transplanted group. We think that the cardiac function of the Flk1$^+$ mGS cell transplanted group was significantly improved through these hypothetical mechanisms. Above these insights, we expect both the effect of angiogenesis and the reduction effect of senescence simultaneously from Flk1$^+$ mGS transplantation *in vivo* when we can improve the method of the cell transplantation to ischemic heart.

In conclusion, the transplanted Flk1$^+$ mGS cells improved the cardiac function in the AMI model mice and we observed that these cells differentiate into cardiomyocytes and endothelial cells. In addition, they prevented host cardiomyocytes death mainly through inhibition of senescence. Of course, these mechanisms require further investigation. When these mechanisms become more clearly elucidated, we hope that in the pluripotent or multipotent stem cells which are available for clinical application of cardiac regeneration therapy, Flk1$^+$ mGS cell transplantation will have advantage in the therapy for AMI patients.

Conflict of Interest

None.

Acknowledgments

We thank Dr. Kodama for kindly providing the OP-9 stromal cell line. This study was supported by the Program for Promotion of Fundamental Studies in Health Science of the National Institute of Biomedical Innovation (NIBIO) (03-2) and Research of Japan and by a Grant-in-Aid for Creative Scientific Research (13GS0009).

References

[1] S.W. Etoch, S.C. Koenig, M.A. Laureano, et al., Results after partial left ventriculectomy versus heart transplantation for idiopathic cardiomyopathy, J. Thorac. Cardiovasc. Surg. 117 (5) (1999) 952–959.
[2] A.A. Kocher, M.D. Schuster, M.J. Szabolcs, et al., Neovascularization of ischemic myocardium by human bone-marrow-derived angioblasts prevents cardiomyocyte apoptosis, reduces remodeling and improves cardiac function, Nat. Med. 7 (4) (2001) 430–436.
[3] A.P. Beltrami, L. Barlucchi, D. Torella, et al., Adult cardiac stem cells are multipotent and support myocardial regeneration, Cell 114 (6) (2003) 763–776.
[4] F.D. Pagani, H. DerSimonian, A. Zawadzka, et al., Autologous skeletal myoblasts transplanted to ischemia-damaged myocardium in humans. Histological analysis of cell survival and differentiation, J. Am. Coll. Cardiol. 41 (5) (2003) 879–888.
[5] S. Baba, T. Heike, M. Yoshimoto, et al., Flk1(+) cardiac stem/progenitor cells derived from embryonic stem cells improve cardiac function in a dilated cardiomyopathy mouse model, Cardiovasc. Res. 76 (1) (2007) 119–131.
[6] A.A. Kocher, M.D. Schuster, N. Bonaros, et al., Myocardial homing and neovascularization by human bone marrow angioblasts is regulated by IL-8/Gro CXC chemokines, J. Mol. Cell. Cardiol. 40 (4) (2006) 455–464.
[7] S.I. Nishikawa, S. Nishikawa, S. Hirashima, et al., Progressive lineage analysis by cell sorting and culture identifies FLK1+VE-cadherin+ cells at a diverging point of endothelial and hemopoietic lineages, Development 125 (9) (1998) 1747–1757.
[8] M. Iida, T. Heike, M. Yoshimoto, et al., Identification of cardiac stem cells with FLK1, CD31, and VE-cadherin expression during embryonic stem cell differentiation, FASEB J. 19 (3) (2005) 371–378.
[9] M. Kanatsu-Shinohara, K. Inoue, et al., Generation of pluripotent stem cells from neonatal mouse testis, Cell 119 (7) (2004) 1001–1012.
[10] S. Baba, T. Heike, K. Umeda, et al., Generation of cardiac and endothelial cells from neonatal mouse testis-derived multipotent germline stem cells, Stem Cells 25 (6) (2007) 1375–1383.
[11] M. Hirashima, H. Kataoka, S. Nishikawa, et al., Maturation of embryonic stem cells into endothelial cells in an *in vitro* model of vasculogenesis, Blood 93 (4) (1999) 1253–1263.
[12] M. Ogawa, M. Kizumoto, S. Nishikawa, et al., Expression of alpha4-integrin defines the earliest precursor of hematopoietic cell lineage diverged from endothelial cells, Blood 93 (4) (1999) 1168–1177.
[13] T. Minamino, T. Yoshida, K. Tateno, et al., Ras induces vascular smooth muscle cell senescence and inflammation in human atherosclerosis, Circulation 108 (18) (2003) 2264–2269.
[14] T. Minamino, H. Miyauchi, T. Yoshida, I. Komuro, Endothelial cell senescence in human atherosclerosis: role of telomeres in endothelial dysfunction, J. Cardiol. 41 (1) (2003) 39–40.
[15] C. Chimenti, J. Kajstura, D. Torella, et al., Senescence and death of primitive cells and myocytes lead to premature cardiac aging and heart failure, Circ. Res. 93 (7) (2003) 604–613.
[16] A. Gonzalez, M. Rota, D. Nurzynska, et al., Activation of cardiac progenitor cells reverses the failing heart senescent phenotype and prolongs lifespan, Circ. Res. 102 (5) (2008) 597–606.
[17] B.D. Chang, Y. Xuan, E.V. Broude, et al., Role of p53 and p21waf1/cip1 in senescence-like terminal proliferation arrest induced in human tumor cells by chemotherapeutic drugs, Oncogene 18 (34) (1999) 4808–4818.
[18] X. Zhang, J. Li, D.P. Sejas, Q. Pang, The ATM/p53/p21 pathway influences cell fate decision between apoptosis and senescence in reoxygenated hematopoietic progenitor cells, J. Biol. Chem. 280 (20) (2005) 19635–19640.
[19] G.V. Silva, E.C. Perin, H.F. Dohmann, et al., Catheter-based transendocardial delivery of autologous bone-marrow-derived mononuclear cells in patients listed for heart transplantation, Tex. Heart Inst. J. 31 (3) (2004) 214–219.
[20] N. Hattan, H. Kawaguchi, K. Ando, et al., Purified cardiomyocytes from bone marrow mesenchymal stem cells produce stable intracardiac grafts in mice, Cardiovasc. Res. 65 (2) (2005) 334–344.
[21] M.A. Laflamme, K.Y. Chen, A.V. Naumova, et al., Cardiomyocytes derived from human embryonic stem cells in pro-survival factors enhance function of infarcted rat hearts, Nat. Biotechnol. 25 (9) (2007) 1015–1024.
[22] Y. Yamada, S. Yokoyama, X. Wang, et al., Cardiac stem cells in brown adipose tissue express CD133 and induce bone marrow nonhematopoietic cells to differentiate into cardiomyocytes, Stem Cells 25 (2007) 1326–1333.
[23] M.D. Schuster, A.A. Kocher, T. Seki, et al., Myocardial neovascularization by bone marrow angioblasts results in cardiomyocyte regeneration, Am. J. Physiol. Heart Circ. Physiol. 287 (2) (2004) H525–H532.